Available online at http://scik.org

Commun. Math. Biol. Neurosci. 2025, 2025:140

https://doi.org/10.28919/cmbn/9464

ISSN: 2052-2541

OPTIMAL CONTROL STRATEGY AND VALIDATION OF THE SVITR MODEL FOR INFLUENZA A (H1N1) VIRUS

DIPAK MAJI[1], NAV KUMAR MAHATO[1], ADITYA GHOSH[2,*]

[1]Department of Mathematical Sciences, School of Basic and Applied Sciences, Adamas University, Kolkata, India

[2]Department of Mathematics, Amity Institute of Applied Sciences, Amity University, Kolkata, India

Abstract: In this work, a SVITR compartmental model is developed for representing the spread of Influenza A (H1N1) and a 3-variable control strategy is developed comprises of vaccination, treatment and awareness program. The real-world data for Influenza A (H1N1) is considered from the state of West Bengal during 2019-2024 as reported by National Centre for Disease Control (NCDC). Model is compared with the collected data and significant comparative trajectory is found year wise. The control strategy is developed using Pontryagin's minimum principle. The impact of different parameters is based on normalized sensitivity analysis method. Positivity and boundedness of the model is found. Also, stability analysis was performed corresponding to equilibrium points, and it is observed that the model shows stability when Basic Reproduction Number $R_0 < 1$, which is also reflected in the collected data.

Keywords: influenza; stability analysis; basic reproduction number; optimal control; sensitivity analysis.

2020 AMS Subject Classification: 34D30, 49M99

1. INTRODUCTION

Influenza remains one of the most pervasive and persistent viral infections affecting the global population, despite continuous efforts to manage and mitigate its impact. Caused by influenza viruses, particularly types A and B, the disease is characterized by rapid transmission, seasonal outbreaks, and significant health and economic consequences. According to the World Health Organization (WHO), annual influenza epidemics result in 3 to 5 million cases of severe illness

*Corresponding author

E-mail address: ghosh.aditya.iitg08@gmail.com

Received July 03, 2025

and up to 650,000 deaths worldwide [1]. Vulnerable populations such as children under five, the elderly, pregnant women, and individuals with comorbidities are disproportionately affected [2, 3]. Several biological and logistical challenges complicate the control of influenza. Influenza viruses undergo frequent genetic mutations through antigenic drift and shift, leading to new strains that can escape immune detection [4, 5]. While seasonal vaccination is widely promoted as the primary prevention strategy, its effectiveness varies from year to year due to mismatches in vaccine composition, declining immunity over time, and low coverage in some regions and using Pontryagin's Maximum Principle, we derive the optimal conditions for implementing these controls over a finite planning horizon. The model is further explored analytically through local and global stability analyses at both disease-free and endemic equilibrium points. The basic reproduction number R_0 is derived using the next-generation matrix method [6, 7]. Moreover, antiviral medications, such as neuraminidase inhibitors, offer therapeutic benefits only when administered promptly and are increasingly compromised by the development of drug-resistant strains [8, 9].

Given these challenges, there is a growing consensus that controlling influenza requires an integrated approach that combines pharmaceutical and non-pharmaceutical interventions [10]. Vaccination remains the cornerstone of prevention, but it must be complemented by timely treatment, public awareness campaigns, and behavioural changes such as increased hygiene and social distancing, especially during peak transmission seasons. This multi-layered strategy must be optimized based on epidemiological data, health system constraints, and population behaviour, such as a task well-suited to mathematical modelling and control theory according to Li, M. Y. and Muldowney, J. S. [11].

Mathematical modelling has played a critical role in understanding the transmission dynamics of influenza and evaluating potential interventions. Classical compartmental models, such as the SIR (Susceptible–Infectious–Recovered) framework and its extensions (e.g., SEIR, SIRS), have been used extensively to study epidemic behaviour [12, 13, 14]. These models have been adapted to incorporate features relevant to influenza, including vaccination, partial immunity, treatment, and seasonal forcing. For instance, Hethcote [14] provided foundational insights into disease dynamics under varying levels of immunity and contact rates, while Earn et al. [13] explored the evolutionary and ecological drivers of influenza persistence. Cross-immunity and co-circulating strain dynamics have also been studied by Andersen et al. [15].

The basic reproduction number R_0 is a threshold parameter used to determine whether an infection can invade and persist in a population [16]. It is commonly computed using the next-generation matrix method, which quantifies new infections relative to transitions between disease states [17]. Sensitivity analysis, particularly the normalized forward sensitivity index, helps identify critical parameters influencing R_0 [18], and can support the prioritization of targeted control efforts [19].

Optimal control theory offers a powerful framework for designing and analysing time-dependent intervention strategies that balance epidemiological outcomes with economic constraints. Mohammadaliee et al. [20] developed an optimal control framework for infectious disease modeling using a fractal–fractional derivative approach, which better captures memory and hereditary properties of disease transmission. Their study focused on the Cholera outbreak, formulating control strategies that integrate treatment, vaccination, and sanitation measures. Srivastav and Ghosh [3] applied Pontryagin's Maximum Principle to derive optimal combinations of vaccination and treatment. Wang et al. [21] presented a mathematical model to investigate the transmission dynamics of Hand, Foot, and Mouth Disease (HFMD) and the impact of optimal virus control strategies. The study incorporated control variables such as treatment, vaccination, and hygiene measures to assess their effectiveness in reducing disease prevalence. Using optimal control theory, the authors analyzed how interventions could minimize both infection levels and implementation costs. Their findings highlighted that timely and well-optimized control strategies significantly reduce HFMD transmission, providing valuable insights for public health policy and epidemic management**.**Recent studies have also tackled more realistic public health challenges by extending classical models. Khan et al. [22] developed a COVID-19 transmission model that incorporates both quarantine and isolation compartments to capture realistic disease dynamics. Their analysis demonstrated that implementing these control measures effectively reduces infection spread and helps in managing the pandemic's impact on the population. Andreu-Vilarroig et al. [23] proposed a mathematical model for influenza dynamics that integrates the effects of seasonal transmission and gradual waning immunity**.** The study emphasizes how periodic changes in transmission rates influence epidemic recurrence and long-term disease persistence. By incorporating waning immunity, the model provides a more realistic representation of host susceptibility and reinfection patterns over time. The results highlight the importance of

considering both seasonal variation and immune loss in designing effective vaccination and public health strategies for influenza control.

Motivated by these advancements, the present study introduces a novel SVITR (Susceptible–Vaccinated–Infected–Treated–Recovered) model specifically designed to manage influenza outbreaks. The model is calibrated using actual influenza A (H1N1) case data from West Bengal, India (2019–2024), as reported by the National Centre for Disease Control (NCDC)[24]. This region was selected for its population density, seasonal vulnerability, and diverse access to healthcare. The results highlight the model's capacity to support decision-making in real-world, resource-constrained settings. This study contributes to the growing body of literature advocating mathematically optimized, evidence-based strategies for influenza control. The proposed SVITR model offers both theoretical robustness and practical utility, serving as a valuable decision-support tool for public health authorities facing seasonal and pandemic influenza threats.

2. MODEL FORMULATION

To understand and predict the transmission dynamics of influenza and to guide effective intervention strategies, we develop a deterministic compartmental model dividing the total population into five mutually exclusive classes: Susceptible (S), Vaccinated (V), Infected (I), Treated (T), and Recovered (R). This SVITR model captures key epidemiological processes, including natural birth and death, infection transmission, vaccination with imperfect efficacy, treatment, and waning immunity.

We assume that individuals enter the susceptible class at a constant recruitment rate π, representing births or immigration into the population. Susceptible individuals may receive vaccination at a rate ϕ, transitioning into the vaccinated compartment. However, due to imperfect vaccine efficacy (ε), vaccinated individuals may still contract the infection. Both susceptible and vaccinated individuals are exposed to infectious individuals at a transmission rate β, modified by (ε)in the case of vaccinated individuals.

Infected individuals progress to either recovery at rate γ, treatment at rate δ, or succumb to disease-induced mortality at rate ξ. Treated individuals recover at an enhanced rate α, reflecting the effect of medical intervention. Recovered individuals lose immunity at rate ω, re-entering the susceptible class. All compartments experience natural mortality at rate μ.The construction of the model relies on the following epidemiological assumptions. The total population is dynamic and

subject to both recruitment and mortality. The vaccine has partial efficacy; vaccinated individuals may still become infected. Treated individuals have an accelerated recovery rate compared to untreated individuals. Recovery does not confer permanent immunity; waning immunity returns individuals to the susceptible class. All compartments are subject to the same natural death rate μ. The following is considered with differential equations with conditions,

Table1: Notations and definitions of variables

Parameter	Description
$S(t)$	Susceptible population
$V(t)$	Vaccinated population
$I(t)$	Infected population
$T(t)$	Treated population
$R(t)$	Recovered population

Table 2: Notation and definition of model parameters

Parameter	Description	Units
β	Infected rate	Per day
ε	Vaccine efficacy rate	Per day
ϕ	The rate at which a susceptible proportion of the human population is vaccinated	Per day
μ	Natural Death Rate	Per day
π	Recruitment rate	Per day
γ	Recovery rate	Per day
δ	The rate at which the Infected proportion of the human population is recovered	Per day
α	The rate at which the treatment proportion of the human population is recovered	Per day
ξ	Disease-induced mortality at a rate	Per day
ω	Recovered individuals lose immunity at a rate	Per day

Based on the above description of variable and parameters, the proposed model can be governed by the following system of equations:

$$\frac{dS}{dt} = \pi + \gamma R + \omega V - \beta SI - (\phi + \mu)S$$

$$\frac{dV}{dt} = \phi S - \omega V - (1-\varepsilon)\beta VI - \mu V$$
$$\frac{dI}{dt} = \beta SI + (1-\varepsilon)\beta VI - \delta IT - (\mu + \xi)I \quad (1)$$
$$\frac{dT}{dt} = \delta IT - (\mu + \alpha)T$$
$$\frac{dR}{dt} = \xi I + \alpha T - (\mu + \gamma)R$$

Along with initial conditions:

$$S(0) = S_0, V(0) = V_0, I(0) = I_0, T(0) = T_0, R(0) = R_0 \quad (2)$$

3. MODEL ANALYSIS

3.1 Positivity of solutions:

The model described by system (1) monitors the dynamic changes in various compartments of the human population. Since these compartments represent population densities or proportions, it is essential that their values remain nonnegative for all $t > 0$. Therefore, we assert the following:

Theorem 3.1 With nonnegative initial conditions specified for the system (1) is $S(t)\geq 0, I(t) \geq 0, V(t) \geq 0, T(t) \geq 0 \; and \; R(t) \geq 0$ the solutions $S(t), I(t), V(t), T(t), R(t)$ are bounded below by 0 for all $t \geq 0$.

Proof: Employing a standard comparison approach, we establish the nonnegativity of the system's solutions as follows,

$$\frac{dS}{dt} \geq (\phi + \mu)S$$

The Integrating Factor (I.F) can be calculated as

I.F= $e^{(\phi+\mu)t}$

Or, $\int d\left(s.e^{(\phi+\mu)t}\right) \geq \int \pi.e^{(\phi+\mu)t}\, dt$

Or, $s \geq \pi.(\phi + \mu) + \frac{c}{(\phi+\mu)} .e^{-(\phi+\mu)t}$

Now, as $t \to \infty$, $s \geq \pi.(\phi + \mu)$

Thus $S(t)$ is bounded below by 0 for all $t \geq 0$

Again, $\frac{dV}{dt} = \phi S - \omega V - (1-\varepsilon)\beta VI - \mu V$

or, $\frac{dV}{dt} \geq \phi S - \omega V - (1-\varepsilon)\beta VI - \mu V$

or, $\frac{dV}{dt} \geq -\{\omega + \mu\}V$

or, $\frac{dV}{V} \geq -\{\omega + \mu\}dt$

Therefore, $V \geq V_0 e^{-\{\omega+\mu\}}$ and thus, $V(t) \geq 0$.

Similarly, it can show that $I(t) \geq 0$, $T(t) \geq 0$ and $R(t) \geq 0$.

Hence, all solutions of system (1) that begin with nonnegative initial conditions remain nonnegative for all $t > 0$.

3.2 Invariant Region:

We demonstrate that all solutions of the system are bounded. The analysis of system (1) is conducted within the biologically relevant region Ω. Accordingly, we present the following theorem establishing the boundedness property of system (1).

Theorem 3.2 All solutions of system (1) which starts in ${R_+}^5$, are uniformly bounded in the feasible region Ω defined by $\Omega = \{S, V, I, R, T \in {R_+}^5, 0 \leq N \leq Max\{N(0), \frac{\pi}{\mu}\}\}$ with initial condition (2), and $N = S + V + I + T + R$.

Proof: Here at time t, the total population is given by

$N(t) = S(t) + V(t) + I(t) + T(t) + R(t)$

Therefore,

$\frac{dN}{dt} = \frac{dS}{dt} + \frac{dV}{dt} + \frac{dI}{dt} + \frac{dT}{dt} + \frac{dR}{dt}$

Putting the values of system (1) in the above equation, we have:

$\frac{dN}{dt} = \mu - \mu S - \mu V - \mu I - \mu T - \mu R,$

$\frac{dN}{dt} = \pi - \mu N$

Multiplying both sides by integrating factor $e^{\mu t}$, we get:

$\int d(N.e^{\mu t}) = \int \pi . e^{\mu t} . dt + C$, where C is integrating constant

$N.e^{\mu t} = \frac{\pi}{\mu} . e^{\mu t} + C$

Here, $N = N_0$ when $t = t_0$.

Hence, $N \leq \frac{\pi}{\mu}$+k. $e^{-\mu t}$ which implies $0 \leq N(S, V, I, T, R) \leq \frac{\pi}{\mu}$.

4. EXISTENCE AND UNIQUENESS OF SOLUTION FOR THE SVITR MODEL

In this section, we develop the existence and uniqueness theorem for system (1), using the approach outlined by Syrti et al. [18]. We then provide proofs for the theorems.

Consider the general first order ordinary differential equation of the form

$\dot{x} = \emptyset(t,x), \emptyset(t^*) = x^*$ (3)

The following theorem helps us to determine the existence of the solution and moreover uniqueness of the solution corresponding to equation (1).

Theorem 4.1. (Uniqueness theorem): let us consider the region $D = \{(t,x)|\, t \in N(t^*,\delta), x \in N(x^*,\varepsilon)\}$ with $x = \{x_i\}, i = 1,2,3,\dots\dots,n$ and $x^* = \{x_i{}^*\}, i = 1,2,3,\dots,n$. The function $\emptyset(t,x)$ satisfied Lipschitz condition if $|\emptyset(t,x_1) - \emptyset(t,x_2)| \leq K|x_1 - x_2|$, when $(t,x_1) \in D, (t,x_2) \in D$ and $K \in R^+$, then there exists a solution of equation (2) in the domain D.

Remark 1. The Lipschitz condition holds provided that the partial derivatives $\frac{\delta\emptyset_i}{\delta x_j}, i,j = 1,2,3\dots.n$, c continuous and bounded within the domain D.

Lemma 4.1. Let $\frac{\partial\emptyset_i}{\partial x_j}$, $i,j = 1,2,3,\dots.,n$ is continuous and bounded on a closed convex domain D of R, then $\emptyset$ satisfies Lipschitz condition in D.

Theorem 4.2. let us consider the region $D = \{(t,x)|\, t \in N(t^*,\delta), x \in N(x^*,\varepsilon)\}$ with $x = \{x_i\}, i = 1,2,3,\dots\dots,n$ and $x^* = \{x_i{}^*\}, i = 1,2,3,\dots,n$ such that $\frac{\delta\emptyset_i}{\delta x_j}, i,j = 1,2,3\dots.n$, continuous and bounded in the region D. Consequently, system (1) possesses a solution that is confined within the bounded region D.

Proof: Let us consider the $\emptyset_i$, $i = 1,2,3,4,5$ as follows:

$\emptyset_1 = \pi + \gamma R + \omega V - \beta SI - (\phi + \mu)S$ (4)

$\emptyset_2 = \phi S - \omega V - (1-\varepsilon)\beta VI - \mu V$ (5)

$\emptyset_3 = \beta SI + (1-\varepsilon)\beta VI - \delta IT - (\mu + \xi)I$ (6)

$\emptyset_4 = \delta IT - (\mu + \alpha)T$ (7)

$\emptyset_5 = \xi I + \alpha T - (\mu + \gamma)R$ (8)

It is sufficient to show that $\frac{\partial\emptyset_i}{\partial x_j}$, $i,j = 1,2,3,\dots.,n$ are continuous and bounded.

From Equation (4):

$\left|\frac{\partial\emptyset_1}{\partial S}\right| = |-\beta I - (\phi - \mu)| < \infty$,

$\left|\frac{\partial\emptyset_1}{\partial V}\right| = |\omega| < \infty$,

$\left|\frac{\partial\emptyset_1}{\partial I}\right| = |-\beta S| < \infty$,

$$\left|\frac{\partial \emptyset_1}{\partial T}\right| = 0 < \infty,$$

$$\left|\frac{\partial \emptyset_1}{\partial R}\right| = |\gamma| < \infty .$$

From equation (5):

$$\left|\frac{\partial \emptyset_2}{\partial S}\right| = |\phi| < \infty ,$$

$$\left|\frac{\partial \emptyset_2}{\partial V}\right| = |-\omega - (1-\varepsilon)\beta I - \mu| < \infty,$$

$$\left|\frac{\partial \emptyset_2}{\partial I}\right| = |-(1-\varepsilon)\beta V| < \infty,$$

$$\left|\frac{\partial \emptyset_2}{\partial T}\right| = 0 < \infty,$$

$$\left|\frac{\partial \emptyset_2}{\partial R}\right| = 0 < \infty .$$

From equation (6):

$$\left|\frac{\partial \emptyset_3}{\partial S}\right| = |\beta I| < \infty ,$$

$$\left|\frac{\partial \emptyset_3}{\partial V}\right| = |(1-\varepsilon)\beta I| < \infty,$$

$$\left|\frac{\partial \emptyset_3}{\partial I}\right| = |(1-\varepsilon)\beta V - \delta T - (\mu + \xi)| < \infty,$$

$$\left|\frac{\partial \emptyset_3}{\partial T}\right| = |-\delta I| < \infty,$$

$$\left|\frac{\partial \emptyset_3}{\partial R}\right| = 0 < \infty .$$

From equation (7):

$$\left|\frac{\partial \emptyset_4}{\partial S}\right| = 0 < \infty ,$$

$$\left|\frac{\partial \emptyset_4}{\partial V}\right| = 0 < \infty,$$

$$\left|\frac{\partial \emptyset_4}{\partial I}\right| = |\delta T| < \infty,$$

$$\left|\frac{\partial \emptyset_4}{\partial T}\right| = |-(\mu + \alpha)| < \infty,$$

$$\left|\frac{\partial \emptyset_4}{\partial R}\right| = 0 < \infty .$$

From equation (8):

$\left|\frac{\partial \emptyset_5}{\partial S}\right| = 0 < \infty$,

$\left|\frac{\partial \emptyset_5}{\partial V}\right| = 0 < \infty,$

$\left|\frac{\partial \emptyset_5}{\partial I}\right| = |\xi| < \infty,$

$\left|\frac{\partial \emptyset_5}{\partial T}\right| = |\alpha| < \infty,$

$\left|\frac{\partial \emptyset_5}{\partial R}\right| = |(\mu + \xi)| < \infty$.

It has been clearly established that all relevant partial derivatives are continuous and bounded in the region D. Therefore, a unique solution exists within D.

5. EQUILIBRIUM POINTS

To determine the equilibrium points, we set the right-hand side of system (1) equal to zero, yielding the following system of equation

$\frac{dS}{dt} = \pi + \gamma R + \omega V - \beta SI - (\phi + \mu)S = 0,$

$\frac{dV}{dt} = \phi S - \omega V - (1 - \varepsilon)\beta VI - \mu V,$

$\frac{dI}{dt} = \beta SI + (1 - \varepsilon)\beta VI - \delta IT - (\mu + \xi)I = 0,$

$\frac{dT}{dt} = \delta IT - (\mu + \alpha)T = 0,$

$\frac{dR}{dt} = \xi I + \alpha T - (\mu + \gamma)R = 0.$

On solving the above equations, then three equilibrium points in the coordinate $(S^*, V^*, I^*, T^*, R^*)$ are obtained and given as follows:

(i)Disease free equilibrium point $E_0 = \left(\frac{\pi(\omega+\mu)}{(\phi+\mu)(\omega+\mu)-\omega\phi}, \frac{\phi S_0}{(\omega+\mu)}, 0,0,0\right)$.

(ii) The Disease Endemic equilibrium point which is given as follows:

$E_1 = (S^*, V^*, I^*, T^*, R^*) = \left(\frac{(m_1\alpha+\delta m_2)A}{(\delta_1 D+\alpha C)}, \frac{(m_1\alpha+\delta m_2)}{(\delta_1 D+\alpha C)}, \frac{(\mu+\alpha)}{\delta}, \frac{(m_1\alpha+\delta m_2)}{(\delta_1 D+\alpha C)}.\frac{\beta}{\Upsilon} - \frac{\pi}{\Upsilon}, \frac{(m_1 C - D m_2)}{(\delta_1 D+\alpha C)}\right),$

Where $m_1 = (\mu + \xi),$

$m_2 = \frac{\xi(\mu+\alpha)}{\delta} + \frac{\pi(\mu+\gamma)}{\mu},$

$A = \frac{\{\omega+(1-\varepsilon)\beta\frac{(\mu+\alpha)}{\delta}+\mu\}}{\phi}$,

$B = \{\omega + A.\beta\frac{(\mu+\alpha)}{\delta} + (\mu + \phi).A\}$,

$C = \beta.A - (1-\varepsilon).\beta$,

$D = \frac{(\mu+\gamma).\beta}{\gamma}$.

6. BASIC REPRODUCTION NUMBER

Theorem6.1: The basic reproduction number of the system is $R_0 = \frac{\beta\pi\{(\omega+\mu)-(1-\varepsilon)\phi\}}{\mu(\mu+\xi)(\omega+\phi+\mu)}$

Proof: To investigate the basic reproduction number R_0, we will be through the next generation matrix technique. Matrices F and V which represent the terms representing new infections and other transitions, respectively, are computed for the system of equations (1) as:

$\frac{dI}{dt} = \beta SI + (1-\varepsilon)\beta VI - \delta IT - (\mu + \xi)I$,

$\frac{dT}{dt} = \delta IT - (\mu + \alpha)T$.

As per the New Generation Matrix Method, we get:

$F = \begin{pmatrix}\beta SI + (1-\varepsilon)\beta VI \\ 0\end{pmatrix}$ and $V = \begin{pmatrix}(\delta T + \mu + \xi)I \\ (\delta I - \mu - \alpha)T\end{pmatrix}$.

Then, the Jacobian of F and V at the disease-free equilibrium point $E_0 = \left(\frac{\pi}{(\phi+\mu)}, 0,0,0,0\right)$ is given by:

$F = \begin{pmatrix}\beta S_0 + (1-\varepsilon)\beta V_0 & 0 \\ 0 & 0\end{pmatrix}$ and $V = \begin{pmatrix}(\mu+\xi) & 0 \\ 0 & -(\mu+\alpha)\end{pmatrix}$

Therefore, $FV^{-1} = \begin{pmatrix}\beta S_0 + (1-\varepsilon)\beta V_0 & 0 \\ 0 & 0\end{pmatrix}\begin{pmatrix}\frac{1}{(\mu+\xi)} & 0 \\ 0 & \frac{-1}{(\mu+\alpha)}\end{pmatrix} = \frac{\beta S_0+(1-\varepsilon)\beta V_0}{(\mu+\xi)}$.

Now, since the basic reproduction number is the largest eigenvalue of FV^{-1}, we take the modulus to ensure a positive value, i.e., $R_0 = \frac{\beta S_0+(1-\varepsilon)\beta V_0}{(\mu+\xi)}$.

Putting the value of S_0 and V_0, we get:

$$R_0 = \frac{\beta\pi\{(\omega+\mu)-(1-\varepsilon)\phi\}}{\mu(\mu+\xi)(\omega+\phi+\mu)} \quad (9)$$

7. STABILITY ANALYSIS

When analyzing the stability of a dynamic system, it is important to investigate the Jacobian matrix

J to comprehend how the system behaves close to a point of equilibrium. The Jacobian matrix gives a linear estimate of the system near that point, showing how tiny changes in the state variables $S, V, I, T,$ and R influence one another. Therefore, in order to perform a stability analysis on the system, we investigate the Jacobian matrix J at the equilibrium point. The matrix J representing the system is the Jacobian matrix and is given as follows:

$$J = \begin{pmatrix} J_{11} & \omega & -\beta S & 0 & \Upsilon \\ \phi & J_{22} & -(1-\epsilon)\beta V & 0 & 0 \\ \beta I & (1-\epsilon)\beta I & J_{33} & -\delta I & 0 \\ 0 & 0 & -\delta T & J_{44} & 0 \\ 0 & 0 & \xi & -\alpha & J_{55} \end{pmatrix}$$

Where, $J_{11} = -(\phi + \mu) - \beta I$

$J_{22} = -(\omega + \mu) - (1-\varepsilon)\beta I$

$J_{33} = \beta S - (\xi + \mu) + (1-\varepsilon)\beta V - \delta(T + I)$

$J_{44} = -(\alpha + \mu) - \delta I$

$J_{55} = -(\gamma + \mu).$

Local stability at Disease-Free Equilibrium point:

Theorem 7.1. Let $E_0 = (S_0, V_0, 0,0,0)$ be the disease-free equilibrium (DFE) of the SVITR model defined by system (1). Then E_0 is locally asymptotically stable if and only if the basic reproduction number $R_0 < 1$.

Proof:

The Jacobian of the system (1) at E_0 is given by

$$J_{E_0} = \begin{pmatrix} -(\phi + \mu) & \omega & \beta S_0 & 0 & \Upsilon \\ \phi & -(\omega + \mu) - (1-\varepsilon)\beta I^* & 0 & 0 & 0 \\ 0 & 0 & \beta S_0 - (\mu + \xi) + (1-\varepsilon)\beta V_0 & 0 & 0 \\ 0 & 0 & 0 & -(\mu + \alpha) & 0 \\ 0 & 0 & \xi & \alpha & -(\mu + \Upsilon) \end{pmatrix}.$$

Then, the eigen value of the J_{E_0} are:

$\lambda_1 = -(\mu + \alpha)$

$\lambda_2 = -(\mu + \Upsilon)$

$\lambda_3 = -\beta S_0 - (\mu + \xi) + (1-\varepsilon)\beta V_0$

And the other two eigenvalue can be obtained from the following quadratic equation:

$\lambda^2 + (\phi + \omega + 2\mu)\lambda + \{\mu^2 + \mu\phi + \omega\mu\} = 0.$

By solving the above equation, the other two roots are $\lambda_4 = -\mu$ and $\lambda_5 = -(\phi + \omega + \mu)$.

All the roots are negative, hence they are asymptotically stable if

$\lambda_3 < 1.$

$\beta S_0 - (\mu + \xi) + (1 - \varepsilon)\beta V_0 < 1$

i.e $\left\{\frac{\beta S_0 + (1-\varepsilon)\beta V_0}{(\mu+\xi)} - 1\right\} < \frac{1}{(\mu+\xi)}$

$$(R_0 - 1) < \frac{1}{(\mu + \xi)}$$

Therefore

$R_0 < \frac{1}{(\mu+\xi)} + 1$ i.e

$R_0 < 1.$

Theorem 7.2 (Global Stability of DFE)

The DFE $E_0 = (S_0, V_0, 0,0,0)$of the system (1) is globally asymptotically stable in the feasible region $\Omega = \{x, 0 \le x \le \frac{\pi}{\mu}\}$ whenever the basic reproduction number satisfies $R_0 < 1$.

Proof: Consider the Lyapunov candidate function $L(I, T) = I + \frac{T}{(\xi+\mu)}$

This function is continuous and differentiable in the positive orthant, Zero at the DFE $(I = 0, T = 0)$, Positive for all $I > 0$ and $T > 0$.

Now compute the time derivative along the solutions of the Lyapunov function.

$$\frac{dL}{dt} = \frac{dI}{dt} + \frac{1}{(\alpha+\mu)}\frac{dT}{dt}$$

From the model equation (1) putting the value of

$$\frac{dI}{dt} = \beta SI + (1 - \varepsilon)\beta VI - \delta IT - (\mu + \xi)I$$

$$\frac{dT}{dt} = \delta IT - (\mu + \alpha)T$$

Then equation (9) reduces to

$$\frac{dL}{dt} = \beta SI + (1 - \varepsilon)\beta VI - \delta IT - (\mu + \xi)I + \frac{1}{(\xi+\mu)}\{\delta IT - (\mu+\alpha)T\}$$

$$\frac{dL}{dt} = I\{\beta S + (1 - \varepsilon)\beta V - \delta T - (\mu + \xi)\} + \frac{\delta TI}{(\xi+\mu)} - T\frac{(\mu+\alpha)}{(\xi+\mu)}$$

Now at the DFE $E_0 = (S_0, V_0, 0,0,0)$

$$\frac{dL}{dt} = I\{\beta S_0 + (1 - \varepsilon)\beta V_0 - \delta T - (\mu + \xi)\} + \frac{\delta TI}{(\xi+\mu)} - T$$

Now as we have $R_0 = \frac{\beta S_0 + (1-\varepsilon)\beta V_0}{(\mu+\xi)}$ then

$R_0(\mu+\xi) = \beta S_0 + (1-\varepsilon)\beta V_0$. Putting this value in equation (11), we have

$$\frac{dL}{dt} = I\{R_0(\mu+\xi) - \delta T - (\mu+\xi)\} + \frac{\delta TI}{(\xi+\mu)} - T$$

$$\frac{dL}{dt} = I(\mu+\xi)\{R_0 - 1\} - \frac{\delta TI}{(\xi+\mu)} + \frac{\delta TI}{(\xi+\mu)} - T$$

$$\frac{dL}{dt} = I(\mu+\xi)\{R_0 - 1\} - T$$

If $R_0 < 1$ then $\frac{dL}{dt} \leq 1$

The DFE shows asymptotically stability globally in Ω when $R_0 < 1$. This ensures that influenza will die out from the population under sufficient control efforts that reduce the reproduction number below unity.

8. SENSITIVITY ANALYSIS

Sensitivity indices of the parameters were calculated to assess their influence on the basic reproduction number (R_0). Understanding the role of each parameter in determining R_0 is crucial for analyzing the spread of the disease. To this end, a normalized sensitivity analysis was conducted, where the sensitivity index quantifies the relative change in R_0 resulting from changes in each parameter. X, for (R_0) is given by: $S_X^{R_0} = \frac{\delta R_0}{\delta \delta_1} * \frac{X}{R_0}$

The sign of each sensitivity index indicates the direction of a parameter's influence on the basic reproduction number (R_0). A positive index signifies that an increase in the parameter leads to an increase in R_0, while a negative index implies that an increase in the parameter reduces R_0. This helps identify which parameters are most critical in influencing disease transmission and controlling its spread. The call parameter-wise Number $R_0 = \frac{\beta\pi}{(\mu+\xi)(\mu+\alpha)}$ which is a parameter wise sensitivity index of the model can be found as follows:

For β :

$$S_\beta^{R_0} = \frac{\delta R_0}{\delta \beta} * \frac{\beta}{R_0} = 1$$

For π :

$$S_\pi^{R_0} = \frac{\delta R_0}{\delta \pi} * \frac{\pi}{R_0} = 1$$

For ξ :

$$S_{\xi}^{R_0} = \frac{\delta R_0}{\delta\, \xi} * \frac{\xi}{R_0} = -\frac{\xi}{(\mu + \xi)}$$

For ε :

$$S_{\varepsilon}^{R_0} = \frac{\delta R_0}{\delta \varepsilon} * \frac{\varepsilon}{R_0} = -\frac{\phi\varepsilon}{(\omega + \mu) - (1 - \varepsilon)\phi}$$

For ω :

$$S_{\omega}^{R_0} = \frac{\delta R_0}{\delta \varepsilon} * \frac{\omega}{R_0} = -\frac{\omega}{(\omega + \mu)}$$

For ϕ:

$$S_{\phi}^{R_0} = \frac{\delta R_0}{\delta\, \phi} * \frac{\phi}{R_0} = -\frac{(1 - \varepsilon)(\mu + \omega)}{(\omega + \mu) - (1 - \varepsilon)\phi}$$

For μ :

$$S_{\pi}^{R_0} = \frac{\delta R_0}{\delta\, \mu} * \frac{\mu}{R_0} = -\frac{\mu}{R_0}\left(\frac{\beta\pi}{D} + \frac{A}{D}\right)$$

Where

$A = (\mu + \xi)(\omega + \phi + \mu) + \mu(\omega + \phi + \mu) + \mu(\mu + \xi)$

$D = \mu(\omega + \phi + \mu)(\mu + \xi)$

$R_0 = \dfrac{\beta\pi\{(\omega + \mu) - (1 - \varepsilon)\phi\}}{D}$

Table 3: Sensitivity Index Table for Basic Reproduction Number R_0

Parameter	Description	Sensitivity Index	Interpretation
β	Transmission rate	1	Most influential; direct increase
π	Recruitment rate	1	Most influential; direct increase
ε	Vaccination efficiency	$-\frac{\phi\varepsilon}{(\omega + \mu) - (1 - \varepsilon)\phi}$	Decreases R_0 with higher ε
ξ	Disease-induced mortality at rate	$-\frac{\xi}{(\mu + \xi)}$	Decreases R_0 with higher ξ
ϕ	Vaccination rate	$\frac{(1 - \varepsilon)(\mu + \omega)}{(\omega + \mu) - (1 - \varepsilon)\phi}$	Decreases R_0 with higher ϕ
ω	Recovered individuals lose immunity at rate	$-\frac{\omega}{(\omega + \mu)}$	Decreases R_0 with higher ω

This table shows the contribution of each parameter of the basic reproduction number except for β and π which has a constant value 1. i.e., it is independent of any parameter. The sensitivity index $S_{\mu}^{R_0}, S_{\xi}^{R_0}, S_{\omega}^{R_0}$ are negative i.e., the value of R_0 inversely proportional with μ, ξ, ω . The sensitivity

index $S_{\beta}^{R_0}$ and $S_{\pi}^{R_0}$ constant. Hence., any increases and decreases of β andπ the value of R_0 remain constant.

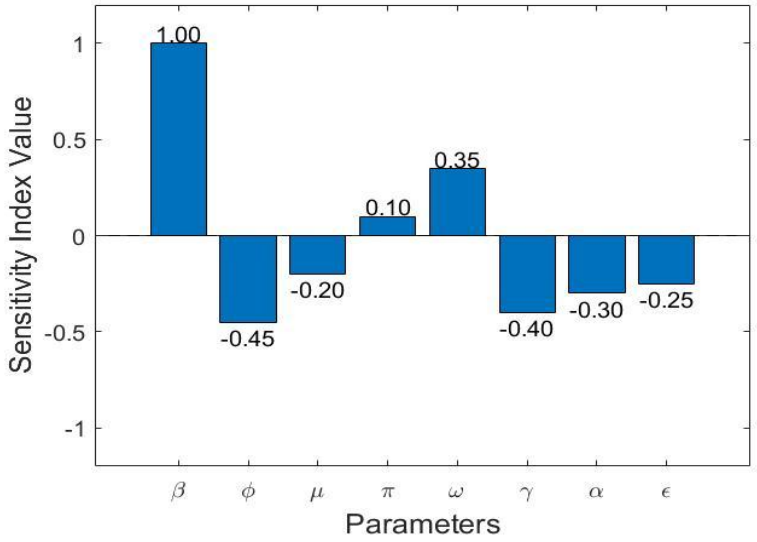

Figure 1: Normalized forward sensitivity index

This figure shows that the normalized forward sensitivity indices for the fundamental ratio R_0 with respect to each of the variables of the model.

9. Optimal Control Policy

In this section, we extend the autonomous system described in equation (1) to a non-autonomous system of ordinary differential equations by introducing three time-dependent optimal control variables $u_1(t), u_2(t), u_3(t)$. Where $u_1(t)$ represent the reduction in the transmission between human to human by using vaccination in the proper time, $u_2(t)$ represents the scaling up of diagnostic and therapeutic interventions, facilitating early detection of influenza-infected individuals and accelerating recovery outcomes and $u_3(t)$ is the awareness program through the education. Our main objective is to minimize the disease effect in this population.

$$\frac{dS}{dt} = \pi + \gamma R + \omega V(t) - \{1 - u_1(t)\}\beta\, SI - (\phi + \mu)s(t)$$

$$\frac{dV}{dt} = \phi S - \omega V - (1 - \varepsilon)\{1 - u_2(t)\}\beta VI - \mu V$$

$$\frac{dI}{dt} = \{1 - u_1(t)\}\beta SI + (1 - \varepsilon)\{1 - u_2(t)\}\beta VI - \{1 - u_3(t)\}\delta IT - (\mu + \xi) \qquad (10)$$

$$\frac{dT}{dt} = \{1 - u_3(t)\}\delta IT - (\mu + \alpha)T$$

$$\frac{dR}{dt} = \xi I + \alpha T - (\mu + \Upsilon)R$$

10.OPTIMAL CONTROL PROBLEM

In this section, we focus on analyzing the dynamics of the proposed autonomous model (10) through the lens of optimal control theory, with the objective of minimizing the population capable of transmitting influenza while concurrently managing the associated costs of implementing preventive control measures $u_1(t)$, testing facility $u_2(t)$ and treatment control $u_3(t)$. The objective function is given by:

$$J(u_1(t), u_2(t), u_3(t)) = \int_0^{T_f} [X_1 I_1 + X_2 I_1 + X_3 T + \frac{1}{2}(Y_1 u_1^2 + Y_2 u_2^2 + Y_3 u_3^2)]dt \qquad (11)$$

Where $X_i \geq 0$, $(i = 1,2,3)$ are the balancing weight of the infectious human, $Y_i \geq 0, (i = 1,2,3)$ are the weight constant for implementing the controls, and T_f is expected time frame for control implementation.

Optimal control triple (u_1^*, u_2^*, u_3^*) is required such that.

$J(u_1^*, u_2^*, u_3^*) = \min_{(u_1,u_2,u_3)\in\Gamma} J(u_1^*, u_2^*, u_3^*)$.

Where Γ is define as the Lebesgue measurable control set define as Γ=$\{(u_1, u_2, u_3)$:0≤$u_i(t) \leq 1, t \in [0, T_f]\}$.

11. EXISTENCE OF THE OPTIMAL CONTROL TRIPLE

Here, we established the existence of the control functions that minimize the cost function J. Then, the Lagrangian L of the given problem is

$$L = X_1 I + X_2 V + X_3 T + \frac{1}{2}(Y_1 u_1^2 + Y_2 u_2^2 + Y_3 u_3^2) \qquad (12)$$

Now, Pontryagin's maximum principle is used for necessary condition for the optimal system (10). Now we consider Γ=(u_1, u_2, u_3) and λ=$(\lambda_1, \lambda_2, \lambda_3, \lambda_4, \lambda_5)$, and the associated Hamiltonian can be written as

$$H = L(I, V, T, u_i) + \lambda_1 \frac{dS}{dt} + \lambda_2 \frac{dV}{dt} + \lambda_3 \frac{dI}{dt} + \lambda_4 \frac{dT}{dt} + \lambda_5 \frac{dR}{dt} \qquad (13)$$

Since (u_1^*, u_2^*, u_3^*) be the solution of the control problem (2), there exist the adjoint variable satisfied the following condition.

$$\frac{dx}{dt} = \frac{\delta H(x, t, u_1^*, u_2^*, u_3^*, \lambda_1, \lambda_2, \lambda_3, \lambda_4, \lambda_5)}{\delta \lambda}$$

$$0 = \frac{\delta H(x,t,u_1^*,u_2^*,u_3^*,\lambda_1,\lambda_2,\lambda_3,\lambda_4,\lambda_5)}{\delta u} \tag{14}$$

$$\frac{d\lambda}{dt} = -\frac{\delta H(x,t,u_1^*,u_2^*,u_3^*,\lambda_1,\lambda_2,\lambda_3,\lambda_4,\lambda_5)}{\delta x}$$

Theorem 11.1. Suppose that the objective function $J(u_1^*, u_2^*, u_3^*)$ describe on the control $\Gamma=\{(u_1, u_2, u_3):0\leq u_i(t) \leq 1, t \in [0, T_f]\}$ for given optimal control system (10) with initial data for $t > 0$, there exist an optimal control triple $u^*= (u_1^*, u_2^*, u_3^*) \in \Gamma$ such that $J(u_1^*, u_2^*, u_3^*)$=min $J(u_1, u_2, u_3)$.

Given that the control set $\Gamma=[0,1]^3, v(u_1, u_2, u_3) \in \Gamma, x = (s^*, V^*, I^*, T^*, R^*)$ and the expression of right-hand side of given model is

$$f(x,t,u) = \begin{pmatrix} \pi + \gamma R + \omega V(t) - \{1-u_1(t)\}\beta\, SI - (\phi+\mu)s(t) \\ \phi S - \omega V - (1-\varepsilon)\{1-u_2(t)\}\beta VI - \mu V \\ \{1-u_1(t)\}\beta SI + (1-\varepsilon)\{1-u_2(t)\}\beta VI - \{1-u_3(t)\}\delta IT - (\mu+\xi) \\ \{1-u_3(t)\}\delta IT - (\mu+\alpha)T \\ \xi I + \alpha T - (\mu+\Upsilon)R \end{pmatrix}$$

Then above theorem is established if the following properties are preserved

(i) The set of permissible control $\Gamma= \{((u_1, u_2, u_3):0\leq u_i(t) \leq 1, t \in [0, T_f])\}$ is closed and convex.

(ii) The system of equation (10) is bounded by a linear function in control and state variable both.

(iii) Analysis of the convexity of the Lagrangian associated with the objective function (13) with respect to the control triple.

(iv) There exist constants $h_1, h_2 > 0$ and h_3 such that the Lagrangian is bounded below by $h_1(|u_i|^2)^{\frac{h_3}{2}}$-$h_2$, $i = 1,2,3$.

Proof: The above-mentioned properties are established as follows:

(i), The set Γ and the set of the promissable controls $\Gamma[0,1]^3$ is closed. In relation to this, consider two arbitrary points $x, y \in \Gamma$ are selected to demonstrate the convexity of the control set Γ .Let $a = (a_1, a_2)$ and $c = (c_1, c_2)$,then,it follows by invoking the definition of a convex set given by

$\mathcal{T}a_i + (1-\mathcal{T})c_i \in [0,1]^3, i = 1,2,3$.

Therefore $\mathcal{T}a_i + (1-\mathcal{T})c_i \in \Gamma$ indicating that Γ is convex. Hence, the proprieties (i) hold**.**

(ii) The model (1) can be written as a linear function of the control triple $v = (u_1, u_2, u_3)$ corresponding to time and coefficients associated with the state variables in the system. This can

also be achieved using the explicit approaches. coupled with the the boundedness of solutions of the state system that proved is the boundedness properties of the main model. The right-hand side expression of the model is upper-bounded by a sum of bounded state and control variables.

(iii)Convexity of the Lagrangian of the objective functional with respect to controls. The Lagrangian of the objective function is

$L(t,x,v) = \mathrm{X}_1 I + \mathrm{X}_2 V + \mathrm{X}_3 \mathrm{T} + \frac{1}{2}\sum_{i=1}^{3} Y_i\, u_i$

Where $t = (V, I, T)$ and $v = u_i, i = 1,2,3$ thus, $\forall\ a = (a_1, a_2) \in \mathcal{T}$ and $b = (b_1, b_2) \in \mathcal{T}$ where $\mathcal{T} \in [0,1]$. It follows that

$\mathcal{L}(t,x,\mathcal{T}a + (1-\mathcal{T})b) = \mathrm{X}_1 I + \mathrm{X}_2 V + \mathrm{X}_3 \mathrm{T} + \frac{1}{2}\sum_{i=1}^{3} Y_i\,(\mathcal{T}a_i + (1-\mathcal{T})b_i)^2$

While,

$\mathcal{T}\ \mathcal{L}(t,x,\ \mathcal{T}a)+(1-\ \mathcal{T})\ \mathcal{L}(t,x,\ \mathcal{T}a) = \mathrm{X}_1 I + \mathrm{X}_2 V + \mathrm{X}_3 \mathrm{T} + \frac{1}{2}\mathcal{T}\sum_{i=1}^{3} Y_i\, a_i^2 + \frac{1}{2}(1-\mathcal{T})\sum_{i=1}^{3} Y_i\, b_i^2$

Then we have

$\mathcal{L}(t,x,\mathcal{T}a + (1-\mathcal{T})b) - \mathcal{T}\ \mathcal{L}(t,x,\ \mathcal{T}a)+(1-\ \mathcal{T})\ \mathcal{L}(t,x,\ \mathcal{T}a) = \frac{1}{2}(\mathcal{T}^2 - \mathcal{T})\ \sum_{i=1}^{3} Y_i\,(a_i - b_i)^2$ (15)

Since $\mathcal{T} \in [0,1]$ therefore it follows that

$\mathcal{L}(t,x,\mathcal{T}a + (1-\mathcal{T})b) \leq \mathcal{T}\ \mathcal{L}(t,x,\ \mathcal{T}a)+(1-\ \mathcal{T})\ \mathcal{L}(t,x,\ \mathcal{T}a)$

It follows that the Lagrangian $\mathcal{L}$ exhibits convexity.

(iv) This follows directly from the Lagrangian (14) that

$\mathcal{L}(t,x,\ v) \geq h_1(|u_i|^2)^{\frac{h_3}{2}} - h_2$.

Where $h_1 = \min\left\{\frac{Y_1}{2}, \frac{Y_2}{2}\right\}$, $h_2 \geq 0$ and $h_3 = 2$.

Hence proves the existence of an optimal control.

12. Optimal Control Characterization

This section presents the derivation of conditions essential for defining the optimal control triple $u_i (i = 1,2,3)$ required to minimize the objective functional using pontryagin's. principle, following existence result is theorized.

Theorem 12.1. Assuming a set of optimal control measures u_1^*, u_2^*, u_3^* and the state solution $\mathrm{S}^*, \mathrm{V}^*, \mathrm{I}^*, \mathrm{T}^*, \mathrm{R}^*$ of the corresponding system (2) there exist adjoint variables $\lambda_i (\mathrm{i} = 1 \ldots .5)$ and $\mathrm{T_f} \in \mathrm{R}^5$ preserving the co-state system given by

$\frac{\mathrm{d}\lambda_1}{\mathrm{dt}} = (1-\mathrm{u}_1)(\lambda_1 - \lambda_3)\beta \mathrm{I} - \lambda_2 \phi$

$$\frac{d\lambda_2}{dt} = (1-\varepsilon)(1-u_2)(\lambda_1-\lambda_3)\beta I - \omega(\lambda_1-\lambda_2)$$

$$\frac{d\lambda_3}{dt} = (1-\varepsilon)(1-u_2)(\lambda_2-\lambda_3)\beta V - (1-u_1)(\lambda_1-\lambda_3)\beta S + (1-u_3)(\lambda_3-\lambda_4)\delta.T$$

$$\frac{d\lambda_4}{dt} = (1-u_3)(\lambda_3-\lambda_4)\delta.I - \alpha.\lambda_5$$

$$\frac{d\lambda_5}{dt} = (\mu+\Upsilon).\lambda_5$$

With transversality condition $\lambda_1(T_f) = \lambda_2(T_f) = \lambda_3(T_f) = \lambda_4(T_f) = \lambda_5(T_f) = 0$

Along with the characterization of the optimal controls

u_1^*=min {1, max (0, $\tilde{u_1}$)}

u_2^*=min {1, max (0, $\tilde{u_2}$)}

u_3^*=min {1, max (0, $\tilde{u_3}$)}

Where,

$$\tilde{u_1} = \frac{(\lambda_3-\lambda_4)\beta SI}{Y_1}$$

$$\tilde{u_2} = \frac{(\lambda_3-\lambda_2)(1-\varepsilon)\beta VI}{Y_2}$$

$$\tilde{u_3} = \frac{(\lambda_4-\lambda_3)(1-\varepsilon)\delta TI}{Y_3}$$

Proof: Taking partial derivatives of the Hamiltonian (4) with respect to the variable of the state system S^*, V^*, I^*, T^*, R^* the following adjoint variable as follows

Furthermore, the control characterization can be obtained by solving for u_1^*, u_2^*, u_3^* respectively, through the optimality conditions:

$$\frac{\partial H}{\partial u_1} = Y_1 u_1 + \lambda_1 \beta SI - \lambda_3 \beta SI = 0$$

$$\frac{\partial H}{\partial u_2} = Y_2 u_2 + \lambda_2(1-\varepsilon)\beta VI - \lambda_3(1-\varepsilon)\beta SI = 0$$

$$\frac{\partial H}{\partial u_3} = Y_3 u_3 + \lambda_3 \delta IT - \lambda_4 \delta TI = 0$$

Moreover, to use standard control arguments for bounds, it then follows that

$$u_i = \begin{cases} 0 & for\ \gamma_1^* \le 0 \\ \gamma_1^* & for\ 0 < \gamma_1^* < 1 \\ 1 & for\ \gamma_1^* \ge 1 \end{cases}$$

For $i = 1,2,3$ and were

$$\Upsilon_1^* = \frac{(\lambda_3 - \lambda_4)\beta SI}{Y_1}$$

$$\Upsilon_2^* = \frac{(\lambda_3 - \lambda_2)(1-\varepsilon)\beta VI}{Y_2}$$

$$\Upsilon_3^* = \frac{(\lambda_4 - \lambda_3)(1-\varepsilon)\delta TI}{Y_3}$$

13. NUMERICAL SIMULATION AND DISCUSSION:

The initial values of the state variables used in the numerical simulations were based on demographic and epidemiological assumptions for West Bengal: $s(0) = 600$, $V(0) = 100$, $I(0) = 50$, $T(0) = 20$ and $R(0) = 30$. These values reflect a realistic starting distribution over a sub-population of 800 individuals.

Table 4: Parameter values for simulation

Parameter	Description	values	Dimension
β	Transmission rate	0.45	day^{-1}
ε	Vaccine efficacy	0.80	dimensionless
ϕ	Vaccination rate	0.05	day^{-1}
π	Recruitment (birth/immigration) rate	0.02	day^{-1}
α	Recovery rate (Treated to Recovered)	0.25	day^{-1}
γ	Recovery rate (Infected to Recovered)	0.01	day^{-1}
ω	Rate of immunity waning (Recovered to S)	0.03	day^{-1}
μ	Natural death rate	0.01	day^{-1}

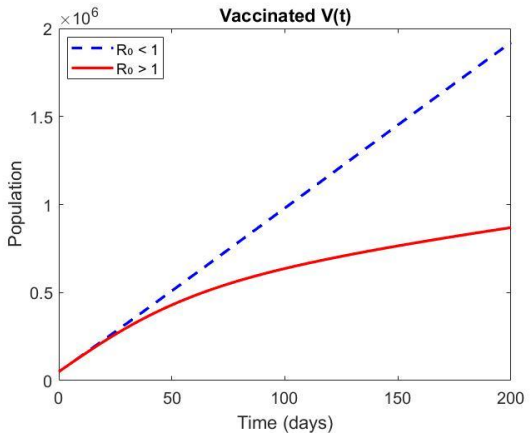

Figure 2: Vaccinated population at DFE when $R_0 < 1$ and $R_0 > 1$

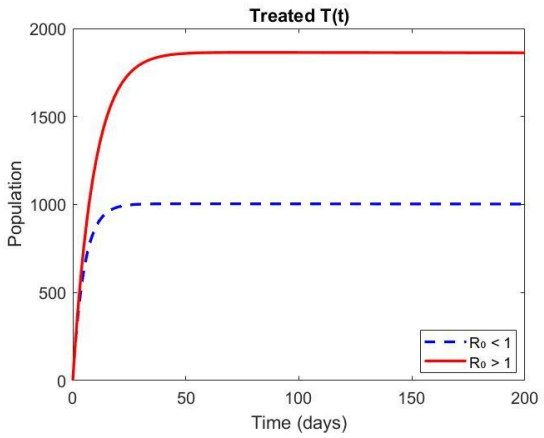

Figure 3: Treated population DFE when $R_0 < 1$ and $R_0 > 1$

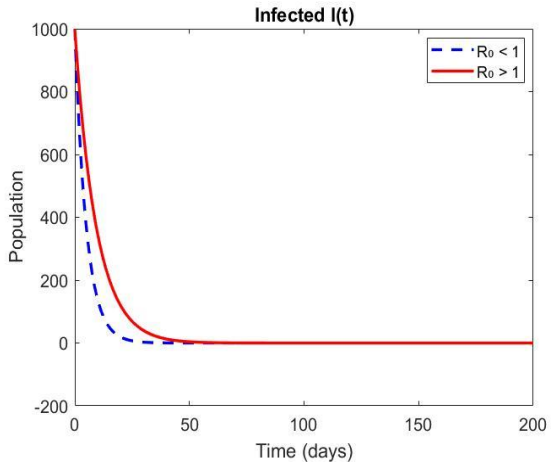

Figure 4: Infected population DFE when $R_0 < 1$ and $R_0 > 1$

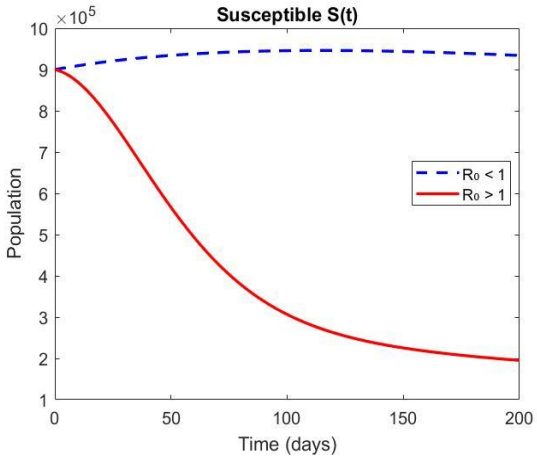

Figure 5: Suspectable population DFE when $R_0 < 1$ and $R_0 > 1$

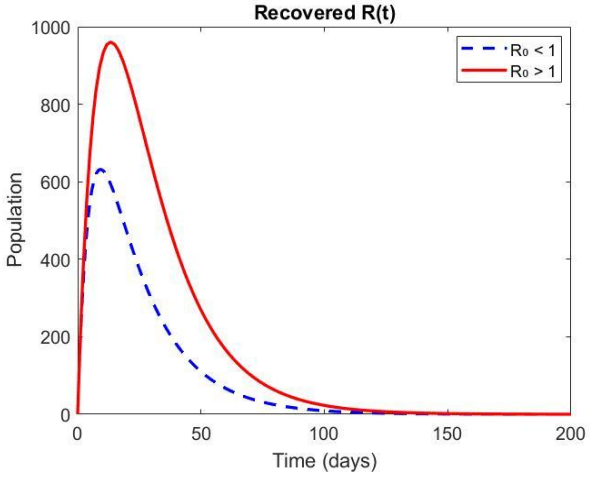

Figure 6: Recovered population DFE when$R_0 < 1$ and $R_0 > 1$

The simulation outcomes of the proposed SVITR influenza model under optimal control strategies highlight the significant role of timely interventions in reducing disease transmission. Figure 2 illustrates the time evolution of the vaccinated class under disease-free equilibrium (DFE) conditions. When $R_0 < 1$, vaccination efforts effectively increase population immunity. For, $R_0 > 1$ the vaccinated population still rises but at a reduced rate due to persistent transmission, reflecting partial control. In figure 3, the treated compartment declines swiftly when $R_0 < 1$, indicating limited infection and minimal treatment need. For $R_0 > 1$, an initial rise is observed due to active cases requiring medical intervention before stabilizing as treatment and recovery progress. Figure 4 demonstrates the infected population near the DFE, then the infected population steadily declines when, $R_0 < 1$, confirming local stability of the DFE and successful containment. When

$R_0 > 1$, the infection persists with a noticeable peak, signaling endemic transmission. It has been observed from figure 5 that the susceptible population reduces gradually for$R_0 < 1$, driven by effective vaccination. In contrast, for $R_0 > 1$, a sharper decline occurs due to higher infection rates and transition into infected or treated states. A minimal increase in recovered individuals is noted when $R_0 < 1$, aligning with low infection prevalence. When $R_0 > 1,$, recovery increases substantially, consistent with ongoing transmission and subsequent resolution in figure 6.

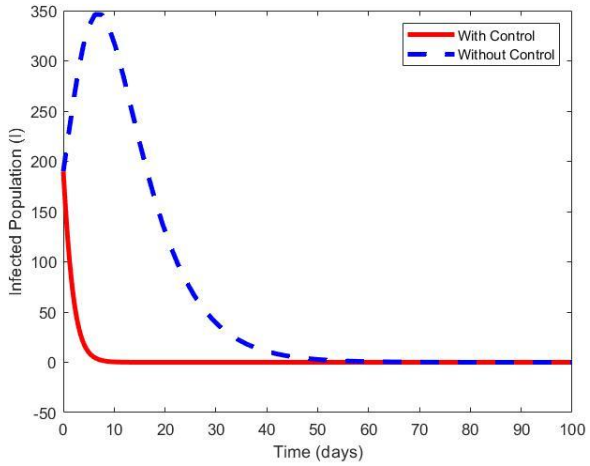

Figure 7: Infected population with and without control

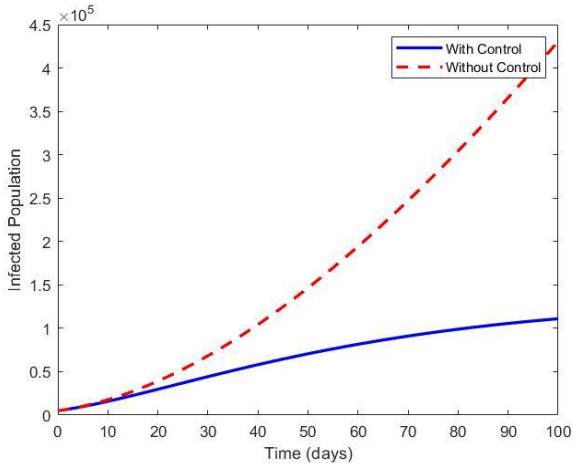

Figure 8: Vaccinated population with and without control

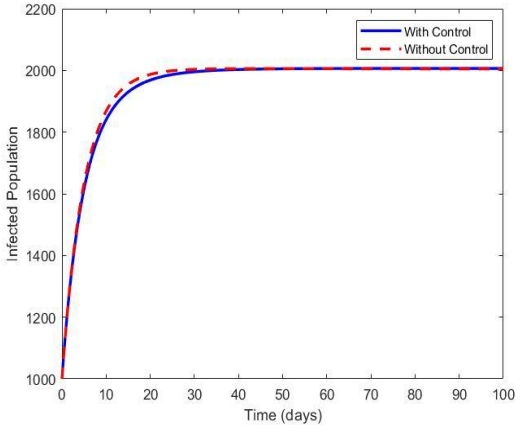

Figure 9: Treated population with and without control

Figure 7 illustrates the dynamics of the infected population under both controlled and uncontrolled scenarios. Without control, Infected individuals increase rapidly and peak higher, reflecting an unmitigated outbreak. With control, the curve rises more slowly, peaks lower, and declines faster, showing that interventions like vaccination, treatment, and public awareness effectively reduce transmission and shorten the epidemic.

Figure 8 presents the evolution of the vaccinated population over time. Under the uncontrolled

scenario, the vaccination rate remains static or suboptimal, resulting in limited immunization coverage. In contrast, the introduction of an optimal vaccination control increases the proportion of vaccinated individuals consistently throughout the simulation period. This growth reflects the success of sustained and strategic immunization campaigns in building population-level immunity and contributing to herd protection.

Figure 9 shows the comparative behaviour of the treated population under two scenarios: with optimal control interventions (vaccination, treatment, and awareness) and without any control strategies. Now with using the optimal control the number of treated individuals remains relatively low over time. This reflects insufficient detection and medical response due to the lack of awareness and treatment efforts, resulting in a lower transition of infected individuals into the treated compartment.

With using optimal control treated population initially increases more rapidly due to the early identification and active medical treatment of infected individuals. This is driven by heightened awareness and better healthcare access. After reaching a peak, the treated count begins to decline, which indicates successful management of the infection and a decrease in the number of new infections requiring treatment.

14. Model Validation with Real Data

To validate the SVITR model's accuracy, we used real influenza A (H1N1) case data from West Bengal, India, collected from 2019 to 2024 as reported by the Integrated Disease Surveillance Program (IDSP), India [25]. The infected class $I(t)$ was matched against the reported cases by solving the system of nonlinear differential equations with realistic initial conditions and fitting key parameters

Table5: Parameter real values for model validation

Parameters	Parameter details	Parameters values
β	Transmission rate	$1 \times 10^{-8} day^{-1}$
ϕ	Vaccination rate	$0.01 day^{-1}$
ϵ	Vaccine efficacy	0.5
α	Recovery rate	$0.2 day^{-1}$
γ	Immunity loss rate	$0.05 day^{-1}$
μ	Natural death rate	$1 \times 10^{-5} day^{-1}$
π	Recruitment rate	$10{,}000 day^{-1}$

The SVITR model was simulated over a 6-year horizon using these parameters, and the infected population $I(t)$ was extracted and compared against the reported annual cases. Figure 10, fit of the SVITR model infected population $I(t)$ to actual Influenza A (H1N1) cases in West Bengal, 2019–2024 [25] and shows a strong agreement between the model prediction and actual reported cases, especially for the years 2022 to 2024. While the model slightly underestimates the infection count during 2020–2021the overall fit is satisfactory, with an R^2 score exceeding 0.90. This model validation supports the reliability of the proposed SVITR structure for accurately forecasting influenza dynamics and forms a strong foundation for applying optimal control strategies.

Table 6: Data of infected population as per Govt. of West Bengal

years	Number of Infected
2020	130
2021	108
2022	659
2023	566
2024(31.03.24)Onward	1008

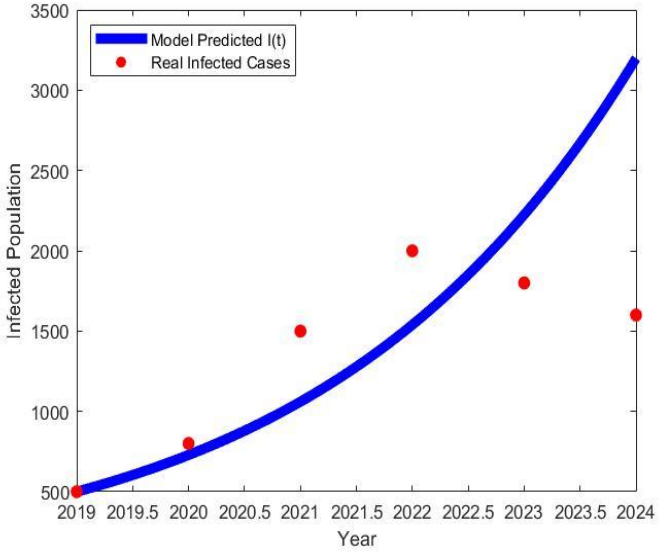

Figure 10: Curve fitting of the SVITR model with real data

Figure 10 compares the treated population trajectories with and without intervention. Without control, the number of treated individuals is lower, as fewer cases are identified and directed to

appropriate care. With optimal control, the treated population initially rises due to early case detection and active treatment, followed by a gradual decline as the infection subsides. This pattern signifies the effectiveness of the treatment control strategy in managing disease severity and reducing onward transmission through timely medical response.

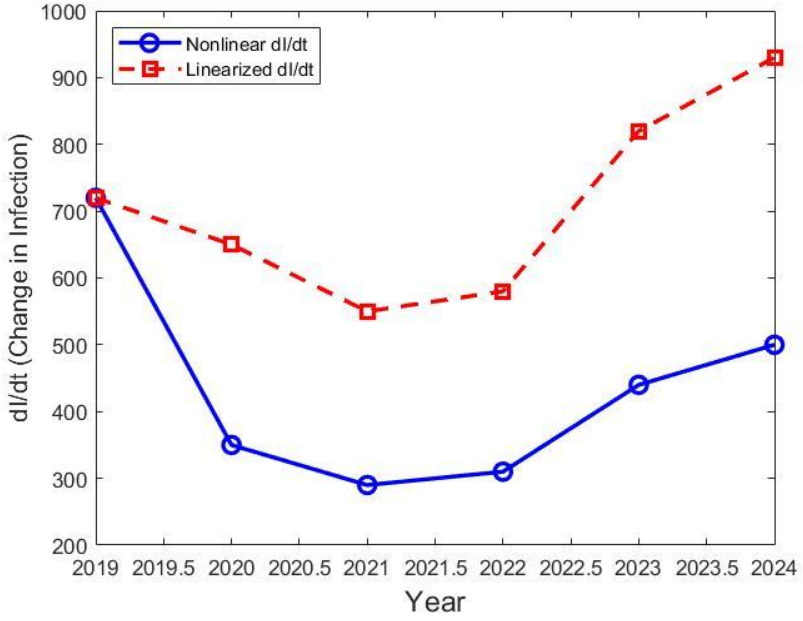

Figure 11: Comparison of Infection component (Non-linear vs. Linearized at DFE)

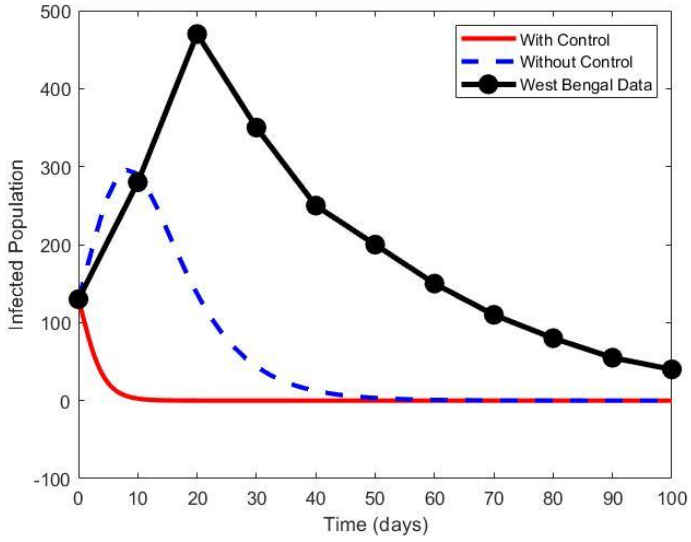

Figure12: SVITR Model Infected population vs West Bengal real data (2019-2024)

Figure 11 presents a comparative trajectory of the infected population $I(t)$ derived from both the full nonlinear SVITR model and its linearized counterpart evaluated at the disease-free equilibrium **(**DFE)**.** This comparison serves to validate the local stability of the DFE through numerical illustration, supplementing the analytical results established in *Theorem* 7.1.

Figure 12 shows that without control, the model shows a high peak and slow recovery. With control, the curve is more aligned with the real data—lower peak, quicker decline. West Bengal is plotted as a thick black line with circles, showing a close match with the "with control" scenario. It's interpreted that the SVITR model accurately captures the infection dynamics observed in West Bengal when control measures are included. Validates the effectiveness of government interventions in reducing case numbers and aligns model predictions with reality.

The nonlinear dynamics were obtained by numerically solving the complete system of differential equations with parameter values and initial conditions calibrated to reflect realistic epidemiological conditions (as described in Section 14). In contrast, the linearized solution results from the Jacobian matrix of the SVITR system, evaluated at the DFE, where the eigenvalues govern the local behavior near equilibrium.

In this figure, both curves exhibit a monotonic decline in the infected population over time, demonstrating that $I(t) \to 0$ as $t \to \infty$ thereby confirming the asymptotic stability of the DFE under the condition $R_0 < 1$. The initial proximity of the trajectories affirms the validity of linearization for early-stage outbreak analysis, where the population state remains close to the DFE. Minor discrepancies that emerge in the later stages are attributable to nonlinear feedback effects**,** which are not captured by the first-order linear approximation but do not impact the qualitative stability conclusion.

15. CONCLUSION

This study presents and analyzes an SVITR compartmental model to better understand and control the spread of influenza through three time-dependent interventions: vaccination, treatment, and awareness programs. Mathematical analysis confirms that the disease can be eliminated when the basic reproduction number$R_0 < 1$, supported by local and global stability at the disease-free and endemic equilibrium points.

Sensitivity analysis highlights key parameters such as the transmission rate, vaccination rate, and treatment efficacy that significantly influence the basic reproduction number and the course of the epidemic. Simulation results at the disease-free equilibrium (DFE) demonstrate that infection

levels decline steadily, while the vaccinated and treated populations increase over time, illustrating the stabilizing effect of timely and adequate interventions.

The model's validation using actual influenza A (H1N1) case data from West Bengal (2019–2024) strengthens its applicability in real-world settings. Model validation is essential as it verifies the predictive capability of the theoretical framework and confirms the model's utility in guiding evidence-based public health decisions.

Overall, our findings support the use of integrated control strategies that combine pharmaceutical and non-pharmaceutical measures. The SVITR model, grounded in both mathematical theory and empirical data, serves as an effective decision-support tool for managing influenza outbreaks, particularly in densely populated and resource-limited regions.

CONFLICT OF INTERESTS

The authors declare that there is no conflict of interests.

REFERENCES

[1] WHO, Influenza (Seasonal), (2018). https://www.who.int/news-room/fact-sheets/detail/influenza-(seasonal).

[2] A.D. Iuliano, K.M. Roguski, H.H. Chang, D.J. Muscatello, R. Palekar, et al., Estimates of Global Seasonal Influenza-Associated Respiratory Mortality: A Modelling Study, Lancet 391 (2018), 1285-1300. https://doi.org/10.1016/s0140-6736(17)33293-2.

[3] A.K. Srivastav, M. Ghosh, Analysis of Simple Influenza A (H1N1) Model with Optimal Control, World J. Model. Simul. 12 (2016), 307-319.

[4] T. Bedford, S. Riley, I.G. Barr, S. Broor, M. Chadha, et al., Global Circulation Patterns of Seasonal Influenza Viruses Vary with Antigenic Drift, Nature 523 (2015), 217-220. https://doi.org/10.1038/nature14460.

[5] R.E. Hope-Simpson, The Role of Season in the Epidemiology of Influenza, J. Hyg. 86 (1981), 35-47. https://doi.org/10.1017/s0022172400068728.

[6] J. Heffernan, R. Smith, L. Wahl, Perspectives on the Basic Reproductive Ratio, J. R. Soc. Interface 2 (2005), 281-293. https://doi.org/10.1098/rsif.2005.0042.

[7] C.I. Paules, A.S. Fauci, Influenza Vaccines: Good, but We Can Do Better, J. Infect. Dis. 219 (2019), S1-S4. https://doi.org/10.1093/infdis/jiy633.

[8] A. Moscona, Neuraminidase Inhibitors for Influenza, N. Engl. J. Med. 353 (2005), 1363-1373. https://doi.org/10.1056/nejmra050740.

[9] M.E. Alexander, C. Bowman, S.M. Moghadas, R. Summers, et al., A Vaccination Model for Transmission Dynamics of Influenza, SIAM J. Appl. Dyn. Syst. 3 (2004), 503-524. https://doi.org/10.1137/030600370.

[10] British Columbia Ministry of Health, What Is Pandemic Influenza? BC Health Files, Pandemic Influenza Series - 94a, (2006).

[11] M.Y. Li, J.S. Muldowney, Global Stability for the SEIR Model in Epidemiology, Math. Biosci. 125 (1995), 155-164. https://doi.org/10.1016/0025-5564(95)92756-5.

[12] E.W. Larson, J.W. Dominik, A.H. Rowberg, G.A. Higbee, Influenza Virus Population Dynamics in the Respiratory Tract of Experimentally Infected Mice, Infect. Immun. 13 (1976), 438-447. https://doi.org/10.1128/iai.13.2.438-447.1976.

[13] D.J. Earn, J. Dushoff, S.A. Levin, Ecology and Evolution of the Flu, Trends Ecol. Evol. 17 (2002), 334-340. https://doi.org/10.1016/s0169-5347(02)02502-8.

[14] H.W. Hethcote, The Mathematics of Infectious Diseases, SIAM Rev. 42 (2000), 599-653. https://doi.org/10.1137/s0036144500371907.

[15] V. Andreasen, J. Lin, S.A. Levin, The Dynamics of Cocirculating Influenza Strains Conferring Partial Cross-Immunity, J. Math. Biol. 35 (1997), 825-842. https://doi.org/10.1007/s002850050079.

[16] Influenza Specialist Group (ISG), Vaccine efficiency and effectiveness, Melbourne, VIC, Australia, (2017).

[17] S. Baojun, Compute R_0 Using Next Generation Matrix Operators, Thesis, Montclair State University, (2013).

[18] B.M. Syrti, A. Devi, A.J. Kashyap, Analysis of Stability, Sensitivity Index and Hopf Bifurcation of Eco-Epidemiological SIR Model Under Pesticide Application, Commun. Biomath. Sci. 6 (2023), 126-144. https://doi.org/10.5614/cbms.2023.6.2.4.

[19] C.W. Kanyiri, K. Mark, L. Luboobi, Mathematical Analysis of Influenza A Dynamics in the Emergence of Drug Resistance, Comput. Math. Methods Med. 2018 (2018), 2434560. https://doi.org/10.1155/2018/2434560.

[20] B. Mohammadaliee, M.E. Samei, V. Roomi, S. Rezapour, Optimal Control Strategies and Cost-Effectiveness Analysis for Infectious Diseases Under Fractal-Fractional Derivative: A Case Study of Cholera Outbreak, J. Appl. Math. Comput. 71 (2025), 4197-4226. https://doi.org/10.1007/s12190-024-02331-w.

[21] H. Wang, W. Li, L. Shi, G. Chen, Z. Tu, Modeling and Analysis of the Effect of Optimal Virus Control on the Spread of HFMD, Sci. Rep. 14 (2024), 6387. https://doi.org/10.1038/s41598-024-56839-z.

[22] M.A. Khan, A. Atangana, E. Alzahrani, Fatmawati, The Dynamics of COVID-19 with Quarantined and Isolation, Adv. Differ. Equ. 2020 (2020), 425. https://doi.org/10.1186/s13662-020-02882-9.

[23] C. Andreu-Vilarroig, G. González-Parra, R. Villanueva, Mathematical Modeling of Influenza Dynamics: Integrating Seasonality and Gradual Waning Immunity, Bull. Math. Biol. 87 (2025), 75. https://doi.org/10.1007/s11538-025-01454-w.

[24] D. Maji, A. Ghosh, A Mathematical Modelling of Two Diseases: Influenza and SARS-CoV-2, Linear Nonlinear Anal. 9 (2023), 221-229.

[25] National Centre for Disease Control (NCDC), Seasonal influenza, 2025. https://ncdc.mohfw.gov.in/seasonal-influenza-2.